

# Transformation of Sulfur Species during Steam/Air Regeneration on a Ni Biomass Conditioning Catalyst

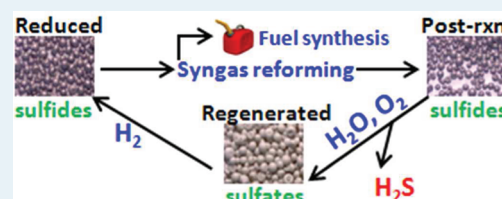
Matthew M. Yung,<sup>†,\*</sup> Singfoong Cheah,<sup>†</sup> Kimberly Magrini-Bair,<sup>†</sup> and John N. Kuhn<sup>‡</sup>

<sup>†</sup>National Renewable Energy Laboratory, Golden, Colorado 80401, United States

<sup>‡</sup>Chemical & Biomedical Engineering, University of South Florida, Tampa, Florida 33620, United States

**ABSTRACT:** Sulfur K-edge XANES identified transformation of sulfides to sulfates during combined steam and air regeneration on a Ni/Mg/K/Al<sub>2</sub>O<sub>3</sub> catalyst used to condition biomass-derived syngas. This catalyst was tested over multiple reaction/regeneration/reduction cycles. Postreaction catalysts showed the presence of sulfides on H<sub>2</sub>S-poisoned sites. Although H<sub>2</sub>S was observed to leave the catalyst bed during regeneration, sulfur remained on the catalyst, and a transformation from sulfides to sulfates was observed. Following the oxidative regeneration, the subsequent H<sub>2</sub> reduction led to a partial reduction of sulfates back to sulfides, indicating the difficulty and sensitivity in achieving complete sulfur removal during regeneration for biomass-conditioning catalysts.

**KEYWORDS:** XANES, nickel, biomass, sulfates, sulfides, regeneration



## 1. INTRODUCTION

Catalyst deactivation and regeneration must be addressed during development of an industrially viable catalyst. These issues are especially relevant in the development of syngas conditioning catalysts used for hydrocarbon and tar reforming, which removes problematic tars and improves carbon efficiency. Although base metal catalysts, such as nickel, are desirable due to their low cost relative to precious metal catalysts, they are susceptible to deactivation during conditioning of biomass-derived syngas by impurities in the feedstocks.<sup>1</sup> Sulfur-containing species, particularly H<sub>2</sub>S, are common catalyst deactivating agents due to the strong chemisorption of sulfur to nickel.<sup>2,3</sup> Biomass-derived syngas may contain 20–600 ppmv H<sub>2</sub>S,<sup>4–6</sup> which results in the deactivation of Ni sites in conditioning catalysts. Therefore, the development of efficient regeneration protocols is necessary for reforming of hydrocarbons in biomass-derived syngas.

Regeneration protocols for sulfur-poisoned nickel, involving steaming to remove sulfur as H<sub>2</sub>S and subsequent reduction in H<sub>2</sub> to reduce NiO to metallic Ni, have been developed and used for reforming catalysts.<sup>7</sup> These techniques have had some success<sup>7</sup> and refinement of the regeneration protocol to decrease the cycle time (i.e., to reduce process downtime), although these may come at the expense of using high operating temperatures that are detrimental to process economics and have other potentially negative impacts on catalyst properties, such as active metal dispersion.<sup>8</sup> A recent study by Li et al. examines various regeneration protocols used for sulfur-poisoned nickel catalysts and shows that there is a great deal of sensitivity to molar ratios of gas components and even flow rates/space velocities.<sup>8</sup> In addition, Li et al. reported a regeneration scheme to remove sulfur from poisoned-Ni catalysts involving a four-step process consisting of (i) controlled oxidation, (ii) thermal decomposition in inert gas,

(iii) H<sub>2</sub>-reduction, and (iv) reaction in H<sub>2</sub>S-free syngas.<sup>8</sup> Although there have been previous studies on regeneration of sulfur-poisoned catalysts, the chemical transformations happening between sulfur and nickel have not been fully observed using the available analytical techniques. Being able to identify these chemical transformations during regeneration can aid in the improvement of regeneration protocols.

The observation of sulfur and nickel species is possible through spectroscopic techniques, including laser Raman spectroscopy,<sup>9–12</sup> X-ray photoelectron spectroscopy (XPS),<sup>10</sup> and X-ray absorption near edge spectroscopy (XANES).<sup>13,14</sup> Each technique has its strengths and weaknesses. For example, depending on the system configuration, Raman spectroscopy is largely a bulk technique and also may not be sensitive enough to detect trace levels of sulfur on a catalyst surface. XPS is surface-sensitive, but requires high surface compositions for detection and is not the preferred method for trace element analysis. The challenge of routinely using XANES is that it requires access to specific equipment at a synchrotron facility. Despite this, XANES is a robust technique capable of unraveling complex material systems, including the one currently under investigation, and is able to differentiate among different species and oxidation states. Chen et al. successfully used XANES to monitor and describe sulfur poisoning mechanisms on Ni and Rh catalysts and were able to identify sulfide, sulfite, and sulfate species.<sup>13</sup> After attempting several techniques<sup>1</sup> (XRD, Raman spectroscopy, energy dispersive spectroscopy, and XPS) to look at sulfur species on postreaction catalysts, we were only able to successfully identify sulfur using XANES. Building on the work by Chen et

Received: March 6, 2012

Revised: May 17, 2012

Published: May 28, 2012

al.<sup>13</sup> and to gain insight into improving regeneration protocols, we aimed to identify if sulfur remained on the biomass-conditioning catalysts following regeneration and determine how the regeneration procedures involving H<sub>2</sub>O and H<sub>2</sub>O + O<sub>2</sub> treatments affected the sulfur species.

## 2. EXPERIMENTAL SECTION

**2.1. Catalyst Synthesis and Characterization.** A commercial, attrition-resistant support (AD90) composed of 90%  $\alpha$ -Al<sub>2</sub>O<sub>3</sub> was used to prepare a 6.1% Ni/2.4% Mg/3.9% K/AD90 catalyst via aqueous impregnation and air calcination at 900 °C as previously described.<sup>1</sup> This catalyst was used for conditioning of biomass-derived syngas at 900 °C and regenerated at 850 °C using H<sub>2</sub>O/O<sub>2</sub>, followed by H<sub>2</sub> reduction.<sup>1</sup> Several other characterization methods, including XRD, H<sub>2</sub> TPR, and Ni K-edge EXAFS were conducted on the samples, and the results have been reported.<sup>1,15</sup> TPR experiments were conducted on 100 mg of catalyst, using 35 sccm of 10% H<sub>2</sub>/Ar and heating at 10 K/min from 50 to 850 °C, with a 30 min hold.

Sulfur K-edge XANES was performed at the Stanford Synchrotron Radiation Lightsource on fresh and spent catalyst samples. The energy range collected was from 2440 to 2600 eV, with 0.1 eV steps from 2460 to 2483 and 2 eV steps outside that range, using a four-element Si drift detector. Merging of individual scans and data reduction were performed with the Athena software package.<sup>16,17</sup> Reference materials of nickel sulfide (NiS), nickel sulfide (Ni<sub>3</sub>S<sub>2</sub>), sodium sulfite (Na<sub>2</sub>SO<sub>3</sub>), and calcium sulfate (CaSO<sub>4</sub>) were analyzed using S K-edge XANES. The XANES spectra of the reference materials showed clear white lines for sulfides (2472 eV), sulfites (2478 eV), and sulfates (2483 eV). These spectra were used for assignments of sulfur species on the catalyst samples along with literature values,<sup>18</sup> but they were not used as quantitative calibration standards.

**2.2. Reaction Testing and Regeneration.** A more detailed description of the pilot-scale reaction experiments, apparatus, and procedures has been previously reported.<sup>1</sup> The raw syngas stream used in the experiments was generated by indirect steam gasification of white oak. Crushed white oak pellets (which contain 125 ppm sulfur in dry basis) were fed at a rate of 15 kg/h along with 15 kg/h of vaporized H<sub>2</sub>O into an 8-in. i.d. fluidized bed reactor filled with olivine at 700 °C. The vapors leaving the gasifier were then sent through a thermal cracker operating at 850 °C to crack the primary pyrolysis products into less complex secondary products and raw syngas. This resulted in a steam-to-total-carbon ratio of ~2 or, neglecting the contribution of CO and CO<sub>2</sub>, a steam-to-reactive-carbon ratio of ~7,<sup>1</sup> with reactive carbon being defined as hydrocarbons and tars. Following the thermal cracker, cyclones were used to remove solids (e.g., char, ash), and the gas phase products were sent to a 14-in. i.d. fluidized bed reactor loaded with 60 kg of the reforming catalyst, where tars and hydrocarbons could undergo steam reforming to produce additional syngas. Ar and He were added to the gas stream as inert tracer gases. A molecular beam mass spectrometer was used to sample this stream and measure tar compositions both before and after the reactor. The gas stream was then sent to a scrubbing unit, where cooled dodecane condensed steam and any remaining tar vapors. Following the scrubber, the composition of the gas stream was measured using Varian gas chromatographs (GCs) and nondispersive infrared (NDIR) detectors before being sent to a thermal oxidizer/vent. The

total gas flow was calculated using helium as an internal standard from its measured concentration and its known molar flow. During the start-up of each reaction cycle, the catalyst reactor was flushed with 1 kg/h N<sub>2</sub> while the process gas leaving the gasifier was diverted and allowed to reach a steady gas composition. The catalyst was kept online until the conversion levels for CH<sub>4</sub>, benzene, or both fell below the technical targets for the experiment, which were conversion of CH<sub>4</sub> ≥ 50%, C<sub>6</sub>H<sub>6</sub> ≥ 90%, and heavy tars ≥ 97%.

Steam/air regeneration and H<sub>2</sub> reduction steps were conducted following raw syngas reforming. Steam (15 kg/h) and nitrogen (3 kg/h) were sent to the reactor at 850 °C, and air was slowly introduced to the stream over the course of ~2 h to obtain the final air flow (0.39 kg/h). The oxidant combination of H<sub>2</sub>O and O<sub>2</sub> was used to regenerate the catalysts by the removal of sulfur poisoned metal sites (M–S + H<sub>2</sub>O ↔ M–O + H<sub>2</sub>S) and oxidation of residual carbon/coke (C + O<sub>2</sub> → CO<sub>2</sub>). The gas phase products leaving the reactor were monitored, and the regeneration procedure continued for 1–1.5 h beyond the time at which H<sub>2</sub>S was no longer detected at the reactor outlet (7–10 h). Measurement of H<sub>2</sub>S concentrations could be reliably performed down to a concentration of 2 ppm. After H<sub>2</sub>O + O<sub>2</sub> regeneration, the catalyst was reduced at 850 °C by exposure to H<sub>2</sub> (0.11 kg/h) and N<sub>2</sub> (11 kg/h) until no further H<sub>2</sub> uptake was measured with the GC and NDIR detectors (~8 h). Catalyst samples (~8–10 g) were taken after each of the reactions, H<sub>2</sub>O + O<sub>2</sub> regeneration, and reduction processes (except for the one following the seventh regeneration), which resulted in <0.5 wt % total catalyst loss via sampling from the original catalyst bed (60 kg). The change in catalyst mass in the reactor was assumed to be negligible during the course of the experiment. Because the catalyst was operated in a fluidized-bed reactor, it was assumed that, on average, the catalyst in the reactor was well-mixed, and it all experienced the same reaction conditions, such that the 10 g catalyst samples were representative of the catalyst within the entire reactor. A summary of the conditions used for the pilot-scale reforming reactions are shown in Table 1.

**Table 1. Process Conditions during Reaction, H<sub>2</sub>O + O<sub>2</sub> Regeneration, and H<sub>2</sub> Reduction**

process	T (°C)	feed conditions
syngas reforming <sup>a</sup>	900	15 kg/h H <sub>2</sub> O, 15 kg/h oak pellets, <sup>a</sup> 1 kg/h N <sub>2</sub>
H <sub>2</sub> O + O <sub>2</sub> regeneration	850	15 kg/h H <sub>2</sub> O, 3 kg/h N <sub>2</sub> , ramp from 0 to 5 SLM air
H <sub>2</sub> reduction	850	11 kg/h N <sub>2</sub> , 20 SLM H <sub>2</sub>

<sup>a</sup>Syngas composition of main constituents (dry, N<sub>2</sub>-free, vol %): 33% H<sub>2</sub>, 24% CO, 22% CO<sub>2</sub>, 13% CH<sub>4</sub>, 3.2% C<sub>2</sub>H<sub>4</sub>, 43 ppm H<sub>2</sub>S, 14 000 mg/Nm<sup>3</sup> total tar (MW > 78), and 1% He (tracer).

Bench-scale catalyst reforming experiments were conducted on a microactivity test system using model syngas with H<sub>2</sub>S to create a series of catalysts that underwent various regeneration treatments. The reforming cycles were conducted at 900 °C, GHSV of 119 000 h<sup>-1</sup>, and steam-to-carbon (S/C) of 7, which corresponded to 62% H<sub>2</sub>O in the gas phase over the catalyst bed for 60 min. The simulated syngas (dry basis) had a composition of 30% H<sub>2</sub>, 30% CO, 18.5% CO<sub>2</sub>, 15% CH<sub>4</sub>, 6.4% C<sub>2</sub>H<sub>4</sub>, 600 ppm C<sub>6</sub>H<sub>6</sub>, and 53 ppm H<sub>2</sub>S. Regeneration was conducted with the same H<sub>2</sub>O content as during the reforming

reaction for 60 min at 850 °C and total GHSV of 114 000 h<sup>-1</sup>. Bench-scale regeneration was with H<sub>2</sub>O, without the addition of O<sub>2</sub>. Following H<sub>2</sub>O regeneration, H<sub>2</sub> reduction was performed at 850 °C in 28% H<sub>2</sub>/N<sub>2</sub> for 60 min to reactivate the catalyst. This approach simulated pilot scale reforming via sequential reforming and regeneration cycles with H<sub>2</sub>S-containing, oak-derived syngas.

### 3. RESULTS AND DISCUSSION

**3.1. Syngas Conditioning Reactions.** The CH<sub>4</sub> conversion during the first two reforming cycles is shown in Figure 1. Conversion of other species, such as benzene and tars, has

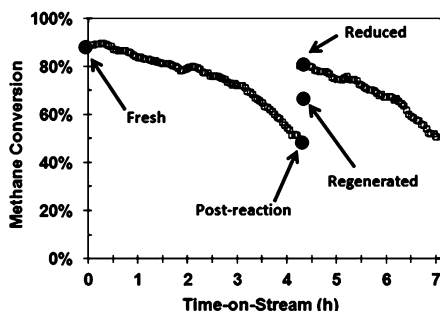


**Figure 1.** Methane conversion during the first cycle of pilot-scale conditioning of biomass-derived syngas at 900 °C and locations where catalyst samples were obtained for XANES analysis.

been reported elsewhere and is not shown here because it is not a good indicator of activity due to high initial conversion levels that were observed.<sup>1</sup> Figure 1 also indicates where catalyst samples were obtained for sulfur XANES analysis (fresh, postreaction, regenerated, and reduced).

During the first 4 h of reaction, the CH<sub>4</sub> conversion decreased from 91% to 50%, which is mainly caused by H<sub>2</sub>S poisoning, as determined by bench-scale control CH<sub>4</sub> steam reforming experiments with and without the presence of H<sub>2</sub>S. When the catalyst had deactivated and a postreaction sample was obtained, the regeneration protocol was then performed. A catalyst sample was obtained following the H<sub>2</sub>O + O<sub>2</sub> regeneration, and then the rest of the catalyst underwent H<sub>2</sub> reduction. Following H<sub>2</sub> reduction, another catalyst sample was obtained for XANES analysis. Figure 2 shows the gas concentrations of H<sub>2</sub>S (NiS + H<sub>2</sub>O = H<sub>2</sub>S + NiO) and H<sub>2</sub>

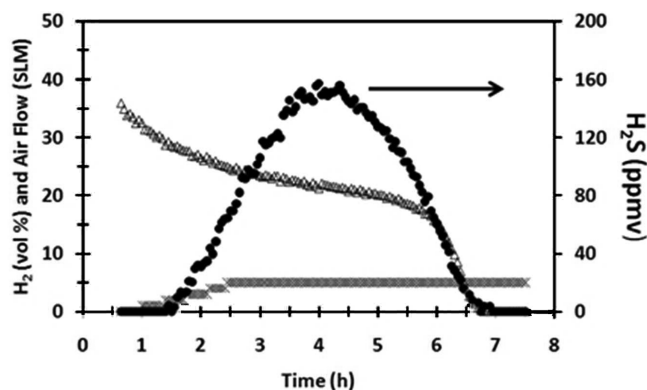


**Figure 2.** Produced gas concentrations of H<sub>2</sub>S (●) and H<sub>2</sub> (Δ), as well as the air flow rate (X), during H<sub>2</sub>O + O<sub>2</sub> regeneration of postreaction nickel catalyst at 850 °C (dry basis).

(Ni + H<sub>2</sub>O = NiO + H<sub>2</sub>) produced during regeneration. The flow rate of air introduced to the reactor is also shown, and it was introduced to help remove any carbon deposits on the catalyst. The regeneration was carried out for 1 h beyond the point when H<sub>2</sub>S could not longer be detected eluting from the reactor, which coincides with the decrease in H<sub>2</sub> generation, indicating that the metallic Ni had been oxidized to NiO. Integration of the H<sub>2</sub>S leaving the reactor indicated that 0.4 (±0.2) mmol of H<sub>2</sub>S/mol Ni left the reactor during each of the regeneration cycles.

XRD of reduced, postreaction, and regenerated samples was conducted and confirmed that the regeneration treatments converted metallic Ni to NiO (with H<sub>2</sub>O + O<sub>2</sub>) and then rereduced NiO to Ni (with H<sub>2</sub>).<sup>1</sup> It was observed that the catalyst deactivated with increasing cycle number, as shown by the decrease in maximum CH<sub>4</sub> conversion during each of the ten reaction cycles displayed in Table 2. This loss of activity coincided with the decrease in the amount of reducible Ni as indicated by TPR (Table 2), which we have previously reported and may be correlated to the formation of an irreducible NiAl<sub>2</sub>O<sub>4</sub> species.<sup>1</sup> Table 2 also shows an increase in the Ni crystallite size with time on-stream, indicating that sintering contributed to some of the loss of activity.

**3.2. Sulfur XANES on Fresh and Spent Catalysts.** The sulfur XANES spectra of the catalysts used for conditioning of oak-derived syngas are shown in Figure 3, which can be used in conjunction with Figure 1 to visualize the points within the process where the catalysts were sampled. The freshly reduced catalyst sample (Figure 3a) does not show the presence of any sulfur species, which is to be expected because the material had not been exposed to any sulfur-containing gases. After the catalyst had been exposed to syngas from biomass gasification and then collected (Figure 3b), a strong sulfide band (2472 eV) and an additional sulfate band (2482 eV) were observed. Because H<sub>2</sub>S can react with metallic nickel to form nickel sulfide, leading to catalyst deactivation, of the presence of a sulfide on the postreaction catalyst confirmed the expected result. The presence of a sulfate band on the postreaction sample likely results from oxidation a sulfide species by H<sub>2</sub>O, although it is not clear if the sulfate species are nickel sulfates, magnesium sulfates, potassium sulfates, or a combination of the species. When the catalyst was regenerated using a mixture of H<sub>2</sub>O and O<sub>2</sub>, sulfur (H<sub>2</sub>S) was observed to leave the catalyst reactor (as shown in Figure 2).

When this regenerated catalyst was analyzed by XANES, it revealed that residual sulfur remained on the catalyst sample. The XANES spectrum of this regenerated catalyst (Figure 3c) shows little or no sulfide contribution, indicating that the treatment of the postreaction catalyst nearly fully removed or transformed the sulfides that were present on the catalyst. The sulfate feature in the XANES spectra, however, persisted between the postreaction and regenerated catalyst samples. As was shown with the reaction and regeneration results in Figure 1 and Figure 2, the regeneration protocol can successfully remove sulfur from the catalyst as H<sub>2</sub>S, and the catalyst is able to recover a significant amount of its activity. The XANES analysis, however, shows that the H<sub>2</sub>O + O<sub>2</sub> regeneration protocol can successfully remove sulfides, but residual sulfates remain on the catalyst. These sulfates are likely due to both (i) a portion of sulfates (which was observed on the postreaction sample) remaining on the catalyst and (ii) an oxidative transformation of sulfides to form sulfates. When the regenerated catalyst was subsequently reduced in H<sub>2</sub> (Figure



**Table 2.** Maximum CH<sub>4</sub> Conversion, Reducibility As Determined by H<sub>2</sub> Consumption during TPR and Ni Crystallite Size Determined Using XRD and the Scherrer Equation during Each of Ten Reaction Cycles for Pilot-Scale Reforming of Biomass-Derived Syngas<sup>1</sup>

	reaction cycle									
	1	2	3	4	5	6	7	8	9	10
X <sub>CH<sub>4</sub>max</sub> (%)	91	82	74	76	70	68	60	65	63	58
reducibility (%)	94	88	85	68	59	62		53	53	47
Ni crystallite size (nm)	38(3)	38(3)	40(3)	38(3)	35(2)	42(3)	44(4)	53(5)	46(3)	

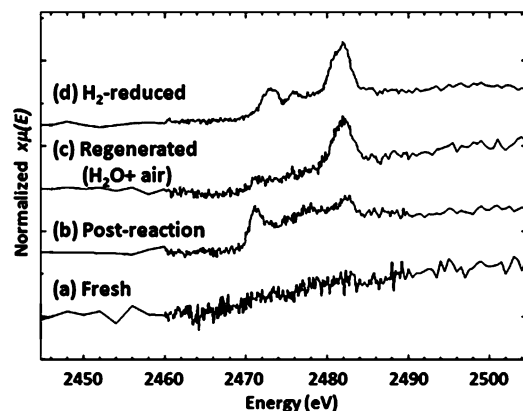


**Figure 3.** Sulfur K-edge XANES spectra of Ni/Mg/K/Al<sub>2</sub>O<sub>3</sub> catalysts used for conditioning of oak-derived syngas at 900 °C and at various stages in the H<sub>2</sub>O + O<sub>2</sub> regeneration and H<sub>2</sub>-reduction processes at 850 °C.

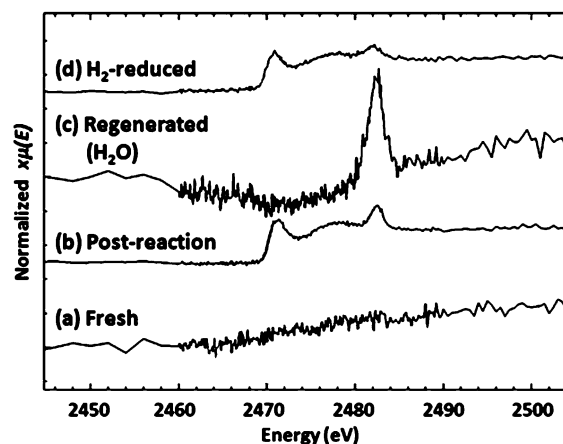


**Figure 4.** Sulfur K-edge XANES spectra of Ni/Mg/K/Al<sub>2</sub>O<sub>3</sub> catalysts used for conditioning a model syngas spiked with H<sub>2</sub>S at 900 °C and at various stages in the H<sub>2</sub>O regeneration and H<sub>2</sub>-reduction processes at 850 °C.

3d) to activate it prior to reaction, there was a partial reduction of the sulfate species to form sulfites (~2477 eV) and sulfides or elemental sulfur (~2473 eV), although the clear presence of sulfates remained.<sup>18</sup> These results indicate that, although sulfur in the form of sulfides is removed from the catalyst through oxidative treatment, a portion of the sulfur may remain as sulfates on the catalyst. A subsequent activation step can then result in readsorption of sulfur as sulfides when nickel becomes reduced.

The pilot-scale regeneration process utilized steam spiked with air to aid in removal of sulfur and carbon deposits on the catalyst, and as such, it was plausible that the air was responsible for the oxidation of sulfides to form sulfates. To test this theory, bench-scale reaction and regeneration experiments were conducted in which the regeneration was carried out in only H<sub>2</sub>O, without the addition of O<sub>2</sub>. The sulfur XANES spectra from the catalysts collected from these experiments are shown in Figure 4. It should be noted that the “fresh” catalyst spectrum is from the same catalyst for both Figures 3 and 4.

Similar to what was observed on the pilot-scale using biomass-derived syngas, the postreaction sample used on the bench scale showed strong sulfide and sulfate white lines (Figure 4b) after exposure to the model syngas stream. When this catalyst was regenerated using H<sub>2</sub>O, the sulfide species were eliminated, though the clear presence of residual sulfates was observed (Figure 4c). The H<sub>2</sub>-reduction of the regeneration catalyst was able to reduce some of the sulfates to sulfides (Figure 4d). Comparing spectra b and d of Figure 4 indicates that some sulfur has been removed through the regeneration process due to the higher signal-to-noise on the postreaction sample, but the same types of sulfur species remain. Although the addition of O<sub>2</sub> during the pilot-scale

regeneration process could still be involved in the oxidation of sulfides to sulfates, these experiments indicate that the presence of H<sub>2</sub>O alone can oxidize sulfides species on the catalyst to form stable sulfates that are difficult to remove.

#### 4. CONCLUSIONS

Direct evidence of the sulfur species found during the reaction and regeneration steps on pilot-scale catalysts used for biomass-derived syngas conditioning was reported for the first time using sulfur K-edge XANES. The regeneration of sulfur-poisoned catalyst using a H<sub>2</sub>O + O<sub>2</sub> regeneration protocol is effective at recovering catalytic activity; however, analysis of the catalyst at various stages within the reaction and regeneration protocol using XANES reveals that the treatment does not fully remove sulfur from the catalyst. The residual sulfur is a contributing factor in the incomplete regeneration of the catalyst, although other processes, such as sintering, phase transformation, and attrition, may also be involved. Regeneration by a H<sub>2</sub>O + O<sub>2</sub> mixture resulted in (i) sulfur removal from the reactor in the form of H<sub>2</sub>S, (ii) mostly complete sulfide removal from the catalyst surface, (iii) formation of sulfates on the catalyst surface, and (iv) oxidation of nickel species to NiO. Subsequent H<sub>2</sub> reduction led to the reduction of NiO to Ni, sulfates were reduced to sulfides, and some catalytic activity was restored. When a H<sub>2</sub>O-only regeneration process was utilized, the same types of surface sulfur species were observed, indicating that the addition of O<sub>2</sub> during regeneration had a negligible effect on the chemistry of the sulfur species.

In summary, the regeneration treatment of H<sub>2</sub>O + O<sub>2</sub> followed by H<sub>2</sub>-reduction was capable of recovering a significant portion of catalyst activity and removing some sulfur from the catalyst bed, but a portion of the sulfur

remained as a poison, transforming from sulfides to sulfates and back to sulfides in a cyclic process. Because short lifetimes are a concern for catalysts used for conditioning biomass-derived syngas prior to the synthesis of liquid fuels, further understanding of how regeneration affects sulfur species found on the catalyst will lead to improved processes and economics. To optimize the regeneration methods further and to obtain insights into the effectiveness of additional steps, such as decomposition under inert gas flow, it would be useful to use sulfur XANES to determine how new, proposed regeneration methods affect sulfur transformation and how they affect the completeness of sulfur removal.

## AUTHOR INFORMATION

### Corresponding Author

\*Address: 1617 Cole Blvd., Golden, CO 80401. Phone: (+1) 303-384-7771. E-mail: matthew.yung@nrel.gov.

### Notes

The authors declare no competing financial interest.

## ACKNOWLEDGMENTS

The authors acknowledge the U.S. Department of Energy, Office of the Biomass Program, contract DE-AC36-99-GO-10337 for financial support and also the staff of the Stanford Synchrotron Radiation Lightsource, particularly Riti Sarangi and Erik Nelson, for use of the facility for XANES experiments. The authors also thank Liyu Li from Pacific Northwest National Laboratory for his valuable suggestions and discussions; Professor Yongshen Chen from Pennsylvania State University for his assistance with the project, through valuable comments and XANES scoping experiments; and Calvin Feik and his team for the collection of spent catalysts used in the pilot plant reactions.

## REFERENCES

- (1) Yung, M. M.; Magrini-Bair, K. A.; Parent, Y. O.; Carpenter, D. L.; Feik, C. J.; Gaston, K. R.; Pomeroy, M. D.; Phillips, S. D. *Catal. Lett.* **2010**, *134*, 242–249.
- (2) Rostrup-Nielsen, J. R.; Sehested, J. *Adv. Catal.* **2002**, *47*, 65.
- (3) Rostrup-Nielsen, J. R. *J. Catal.* **1968**, *11*, 220–227.
- (4) Cheah, S.; Carpenter, D. L.; Magrini-Bair, K. A. *Energy Fuels* **2009**, *23* (11), 5291–5307.
- (5) Carpenter, D. L.; Bain, R. L.; Davis, R. E.; Dutta, A.; Feik, C. J.; Gaston, K. R.; Jablonski, W. S.; Phillips, S. D.; Nimlos, M. R. *Ind. Eng. Chem. Res.* **2010**, *49* (4), 1859–1871.
- (6) Yung, M. M.; Jablonski, W. S.; Magrini-Bair, K. A. *Energy Fuels* **2009**, *23*, 1874–1887.
- (7) Rostrup-Nielsen, J. R. *J. Catal.* **1971**, *271*, 171–178.
- (8) Li, L.; Howard, C.; King, D. L.; Gerber, M.; Dagle, R.; Stevens, D. *Ind. Eng. Chem. Res.* **2010**, *49*, 10144–10148.
- (9) Cheng, Z.; Abernathy, H.; Liu, M. *J. Phys. Chem. C* **2007**, *111*, 17997–18000.
- (10) Kuhn, J. N.; Lakshminarayanan, N.; Ozkan, U. S. *J. Mol. Catal. A: Chem.* **2008**, *282*, 9–21.
- (11) Cheng, Z.; Liu, M. *Solid State Ionics* **2007**, *178*, 925.
- (12) Dong, J.; Cheng, Z.; Zha, S.; Liu, M. *J. Power Sources* **2006**, *156*, 461.
- (13) Chen, Y.; Xie, C.; Li, Y.; Song, C.; Bolin, T. B. *Phys. Chem. Chem. Phys.* **2010**, *12*, 5707–5711.
- (14) Xie, C.; Chen, Y.; Li, Y.; Wang, X.; Song, C. *Appl. Catal., A* **2010**, *390*, 210–218.
- (15) Yung, M. M.; Kuhn, J. N. *Langmuir* **2010**, *26* (21), 16589–16594.
- (16) Ravel, B.; Newville, M. *J. Synchrotron Radiat.* **2005**, *12*, 537–541.
- (17) Newville, M. *J. Synchrotron Radiat.* **2001**, *8*, 322–324.
- (18) Struiss, R. P. W. J.; Schildhauer, T. J.; Czekaj, I.; Janousch, M.; Biollaz, S. M. A.; Ludwig, C. *Appl. Catal., A* **2009**, *362*, 121–128.